

## Fluorescence of a Rotationally Constrained Tryptophan Derivative, 3-Carboxy-1,2,3,4-tetrahydro-2-carboline

Luanne Tilstra,<sup>†</sup> Melissa C. Sattler,<sup>‡</sup> William R. Cherry, and Mary D. Barkley\*

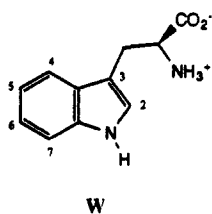
Contribution from the Department of Chemistry, Louisiana State University, Baton Rouge, Louisiana 70803-1804. Received May 18, 1990. Revised Manuscript Received August 10, 1990

**Abstract:** Despite a plethora of work on tryptophan photophysics, the origin of the complex fluorescence decay kinetics is still unknown. A question remains whether the two fluorescence lifetimes of the tryptophan zwitterion are due to ground-state and therefore excited-state heterogeneity resulting from rotameric forms. To test the conformer model, we synthesized a tryptophan derivative, 3-carboxy-1,2,3,4-tetrahydro-2-carboline, which restricts rotation of the alanyl side chain. The constraint limits the number of conformations available to the molecule without greatly affecting the electronic properties. The absorption and emission spectra and the pK of the amino group are similar to those of tryptophan. The fluorescence decay of the constrained derivative is an apparent monoexponential. The zwitterion has a lifetime of  $6.2 \pm 0.2$  ns and the anion has a lifetime of  $4.7 \pm 0.2$  ns at 25 °C. Global analysis of time-resolved emission spectral data for the zwitterion reveals a double-exponential decay, which may reflect two stable conformations of the partially unsaturated six-membered ring. This is discussed in detail in the following paper.

The fluorescence decay of tryptophan has great potential for probing the structure and dynamics of proteins and peptides. A complex fluorescence decay is usually observed for single tryptophans in polypeptide chains, presumably reporting the heterogeneous microenvironment of the chromophore. However, knowledge of the structural and chemical bases of the photophysics is necessary to interpret the fluorescence results. Despite extensive investigation over the past decade by a number of research groups,<sup>1,2</sup> the relationship between tryptophan fluorescence decay and ground-state structure is not well understood.

Indole, the chromophore of tryptophan, has two overlapping electronic transitions in the first absorption band:<sup>3</sup>  ${}^1L_a \leftarrow {}^1A$  and  ${}^1L_b \leftarrow {}^1A$ . The fluorescence emission spectrum of indole is highly sensitive to environment, exhibiting an unusually large Stokes shift in polar solvents. The solvatochromism of indole has been attributed to inversion of the two lowest excited states induced by solvent polarity and solvent relaxation.<sup>4,5</sup> The emitting state changes from  ${}^1L_b$  in nonpolar solvents to  ${}^1L_a$  in polar solvents. The fluorescence quantum yields and lifetimes of indole and its derivatives are very dependent on temperature.<sup>5,6</sup> Several temperature-dependent nonradiative processes, photoionization,<sup>7</sup> excited-state proton transfer,<sup>8,9</sup> and electron transfer,<sup>10,11</sup> can occur depending on the compound and solution conditions. Intersystem crossing is also a major deactivation pathway.<sup>12</sup> The fluorescence decay of indole is a single exponential with a lifetime of 4.9 ns in water at neutral pH.<sup>13,14</sup>

Tryptophan, W, on the other hand, has a double-exponential decay at neutral pH. The major component has a lifetime of 3.1



ns with emission maximum at 350 nm, and the minor component has a lifetime of 0.5 ns with emission maximum at 335 nm.<sup>15</sup> At high pH, the fluorescence quantum yield is increased<sup>16</sup> and a single-exponential decay of  $\sim 9$ -ns lifetime is observed.<sup>17-20</sup> At low pH the quantum yield is decreased<sup>16</sup> and the 3.1-ns component is quenched.<sup>17,18</sup> In the zwitterion only the longer lifetime is temperature dependent.<sup>20</sup> Below 215 K, the decay function collapses to a single exponential with a lifetime of  $\sim 5.3$  ns, and

the emission maximum shifts  $\sim 20$  nm to the blue.<sup>21</sup>

Several models have been proposed to account for the double-exponential decay of the tryptophan zwitterion. An early model invoking dual emission from  ${}^1L_a$  and  ${}^1L_b$  was discarded.<sup>15</sup> Excited-state proton transfer was identified as a nonradiative decay route from the large solvent isotope effect on fluorescence quantum yield and lifetimes.<sup>6,9,13,22</sup> The complex decay was initially ascribed to intramolecular proton transfer involving diffusive encounters of the positively charged amine on the alanyl side chain and the excited indole ring.<sup>17</sup> Further support for intramolecular proton transfer came from the observation of a highly efficient and selective photoinduced hydrogen-exchange reaction at the C4 position of the indole ring.<sup>23</sup> In the proposed mechanism for the photosubstitution reaction, the ammonium loops back over the indole to form a six-membered ring and catalyzes the proton exchange. Subsequent work quantifies the contribution of proton transfer to the nonradiative decay of tryptophan in methanol/water solutions.<sup>24</sup> Another model argues that the complex decay of the tryptophan zwitterion actually represents a distribution of lifetimes rather than distinct components.<sup>25</sup> This distribution may be

- (1) Creed, D. *Photochem. Photobiol.* **1984**, *39*, 537-562.
- (2) Beechem, J. M.; Brand, L. *Annu. Rev. Biochem.* **1985**, *54*, 43-71.
- (3) Valeur, B.; Weber, G. *Photochem. Photobiol.* **1977**, *25*, 441-444.
- (4) Lami, H.; Glasser, N. *J. Phys. Chem.* **1986**, *84*, 59-66.
- (5) Eisinger, J.; Navon, G. *J. Chem. Phys.* **1969**, *50*, 2069-2077.
- (6) Kirby, E. P.; Steiner, R. F. *J. Phys. Chem.* **1970**, *74*, 4480-4490.
- (7) Beni, D. V.; Hayon, E. *J. Am. Chem. Soc.* **1975**, *97*, 2612-2619.
- (8) Vander Donck, E. *Bull. Soc. Chim. Belg.* **1969**, *78*, 69-75.
- (9) Stryer, L. *J. Am. Chem. Soc.* **1966**, *88*, 5708-5712.
- (10) Steiner, R. F.; Kirby, E. P. *J. Phys. Chem.* **1969**, *73*, 4130-4135.
- (11) Ricci, R. W.; Nesta, J. M. *J. Phys. Chem.* **1976**, *80*, 974-980.
- (12) Klein, R.; Tatischeff, I.; Bazin, M.; Santus, R. *J. Phys. Chem.* **1981**, *85*, 670-677.
- (13) Ricci, R. W. *Photochem. Photobiol.* **1970**, *12*, 67-75.
- (14) De Lauder, W. B.; Wahl, Ph. *Biochim. Biophys. Acta* **1971**, *243*, 153-163.
- (15) Szabo, A. G.; Rayner, D. M. *J. Am. Chem. Soc.* **1980**, *102*, 554-563.
- (16) White, A. *Biochem. J.* **1959**, *71*, 217-220.
- (17) Robbins, R. J.; Fleming, G. R.; Beddard, G. S.; Robinson, G. W.; Thislethwaite, P. J.; Woolfe, G. J. *J. Am. Chem. Soc.* **1980**, *102*, 6271-6279.
- (18) Gudgin, E.; Lopez-Delgado, R.; Ware, W. R. *Can. J. Chem.* **1981**, *59*, 1037-1044.
- (19) Gudgin, E.; Lopez-Delgado, R.; Ware, W. R. *J. Phys. Chem.* **1983**, *87*, 1559-1565.
- (20) Boens, N.; Janssens, L. D.; De Schryver, F. C. *Biophys. Chem.* **1989**, *33*, 77-90.
- (21) Gudgin-Templeton, E. F.; Ware, W. R. *J. Phys. Chem.* **1984**, *88*, 4626-4631.
- (22) Lehrer, S. S. *J. Am. Chem. Soc.* **1970**, *92*, 3459-3462.
- (23) Saito, I.; Sugihama, H.; Yamamoto, A.; Muramatsu, S.; Matsuura, T. *J. Am. Chem. Soc.* **1984**, *106*, 4286-4287.
- (24) Shizuka, H.; Serizawa, M.; Shimo, T.; Saito, I.; Matsuura, T. *J. Am. Chem. Soc.* **1988**, *110*, 1930-1934.
- (25) James, D. R.; Ware, W. R. *Chem. Phys. Lett.* **1985**, *120*, 450-454.

<sup>†</sup> Present address: NIST, Bldg. 224, Rm. B-320, Gaithersburg, MD 20899.

<sup>‡</sup> Present address: Dow Chemical USA, R&D Bldg. 2503, Box 400, Plaquemine, LA 70765-0400.

analyzed as a sum of two or three exponentials. However, the data are fitted equally well by discrete or continuous functions and no criteria for choosing the physically significant model are specified.<sup>26</sup>

The prevailing model for tryptophan photophysics is the conformer model.<sup>15,27</sup> This model attributes the double-exponential decay to multiple ground-state rotamers, which do not interconvert during the lifetime of the excited state. The different fluorescence lifetimes of individual rotamers result from quenching by intramolecular proton-<sup>17,23,24</sup> or electron-transfer reactions.<sup>28-30</sup> The elegant time-resolved studies of gas-phase tryptophan analogues cooled in supersonic jets have clearly demonstrated that individual rotamers have monoexponential decays and that the fluorescence lifetimes may differ between rotamers.<sup>31,32</sup> <sup>1</sup>H NMR studies show six conformational rotamers of tryptophan in solution.<sup>33</sup> In the predominant ground-state rotamer the plane of the indole ring is perpendicular to the C<sup>α</sup>-C<sup>β</sup> bond, and the C<sup>α</sup>-C<sup>β</sup> bond is in the *g*(-) conformation (carboxylate anti to indole). While *t* and *g*(+) rotamers (ammonium and α-hydrogen anti to indole) coexist with the *g*(-) rotamer, these less favorable conformations become less stable at higher temperature.<sup>34</sup> For six rotamers to give rise to only two lifetimes, some rotamers must have similar lifetimes or must interconvert on the fluorescence time scale.

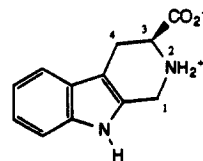
At present, there is no consensus about the relative importance of various rotamers and quenching mechanisms in the tryptophan fluorescence decay. Szabo and Rayner<sup>15</sup> proposed that distinct C<sup>α</sup>-C<sup>β</sup> rotamers ( $\chi_1$  torsion) cause the lifetime heterogeneity. In agreement with the <sup>1</sup>H NMR results, they associated the major 3.1-ns component with the *g*(-) rotamer and the minor 0.5-ns component with the *g*(+) rotamer. Because both rotamers have the ammonium close to the indole ring, these authors favored proton- or electron-transfer quenching processes involving the positively charged amine. The *g*(+) rotamer also has the carboxylate near the indole, which was thought to enhance the quenching. Petrich et al.<sup>28</sup> modified the conformer model and specified that the competing nonradiative process is intramolecular electron transfer from indole to the carboxylate. The enhancement of quantum yield and lifetime by D<sub>2</sub>O was attributed to a slower electron-transfer rate in this solvent. Gudgin-Templeton and Ware<sup>21</sup> suggested that electron transfer to solvent is a competing nonradiative decay pathway. Finally, Engh et al.<sup>30</sup> proposed that rotation about the C<sup>β</sup>-C<sup>γ</sup> bond ( $\chi_2$  torsion) plays an important role in the tryptophan fluorescence decay. Molecular dynamics simulations in vacuum indicate that the C<sup>α</sup>-C<sup>β</sup> rotamers interconvert rapidly compared to the fluorescence lifetime while the C<sup>β</sup>-C<sup>γ</sup> transitions occur more slowly. The authors suggested that the two exponential decays correspond to the two major C<sup>β</sup>-C<sup>γ</sup> rotamers having the indole ring perpendicular to the C<sup>α</sup>-C<sup>β</sup> bond but rotated 180° relative to each other.

The question remains whether the two fluorescence lifetimes of tryptophan in solution are due to ground-state rotamers. Accordingly, we synthesized a tryptophan derivative in which rotations about the C<sup>α</sup>-C<sup>β</sup> and C<sup>β</sup>-C<sup>γ</sup> bonds are restricted by incorporating the amino group into a six-membered ring. The constraint limits the number of conformers available to the molecule without greatly affecting the electronic structure of the chromophore. This paper presents the fluorescence decay results

for the modified tryptophan. The companion paper<sup>35</sup> reports the solution structure of the constrained derivative and discusses the fluorescence quenching mechanism. These results establish for the first time a one-to-one correspondence between fluorescence lifetime and ground-state conformation in a tryptophan derivative.

### Experimental Section

**Synthesis.** 3-Carboxy-1,2,3,4-tetrahydro-2-carboline, W(1), was synthesized in one step from L-tryptophan by modifying the procedure of



W(1)

Harvey et al.<sup>36</sup> A 10.00-g sample of L-tryptophan (Sigma, recrystallized three times from 70% ethanol) was dissolved in 500 mL of 0.1 M NaOH and the resultant mixture reacted with 6 mL of 37% formalin solution by heating at 38 °C. After 15 h, the reaction was cooled to 25 °C and the pH was adjusted to 6.5 with concentrated HCl. The yellow precipitate that formed was filtered, washed with water, and triturated with boiling methanol to remove most of the color. The solid was crystallized from boiling water (solubility 0.17 g/100 mL of H<sub>2</sub>O at 100 °C) after treatment with decolorizing carbon. Two successive recrystallizations gave white plates (4.83 g, 41%); mp 311–311.5 °C uncorrected; Anal. (C<sub>12</sub>H<sub>14</sub>N<sub>2</sub>O<sub>3</sub>) C, N, H calcd 6.02, found, 5.98; <sup>1</sup>H NMR (200 MHz, ref to DSS in D<sub>2</sub>O, pD 11.7)  $\delta$  7.6–7.1 (d, d, m, Ar-H), 4.0 (dd, CH<sub>2</sub>N, <sup>2</sup>*J*(HH) 16.11 Hz), 3.47 (dd, H<sub>X</sub>), 3.06 (dd, H<sub>A</sub>), 2.72 (dd, H<sub>B</sub>). TLC analysis [silica, ethanol/acetonitrile (1:1) and butanol/acetic acid/water (4:1:1)] revealed a single spot when visualized by UV, iodine, and ninhydrin.

**MS/MS.** FAB mass spectrometry was performed on a Finnigan TSQ-70 mass spectrometer, using a neutral beam of Xe atoms with a translational energy of 8 kV. Positive ion mass spectra were obtained from samples prepared in a glycerol matrix. Samples were introduced at the inlet with a probe at ambient temperature. Measurements were based on a calibration standard consisting of glycerol/cesium iodide (1:1 mol/mol). To determine the fragmentation pattern of the molecule, collision-induced dissociation experiments were done on individual ions using Ar. Mass spectrum of W(1) gave ions at *m/z* (relative intensity) 144 (10) and 217 (15) [MH]<sup>+</sup>. Collision-induced dissociation of ion *m/z* 217 gave ions at *m/z* 74 (5), 143 (10), 144 (100), 171 (3), and 217 (7).

**Absorbance.** Absorbance was measured on a Cary 219 spectrophotometer. W(1) was dissolved in 0.01 M phosphate buffer at the indicated pH. Sample absorbance was <0.1 at 280 nm for steady-state fluorescence measurements and <0.2 at 295 nm for time-resolved measurements.

**Steady-State Fluorescence.** Steady-state fluorescence was measured in the ratio mode on an SLM 8000 spectrofluorometer equipped with single excitation (4-nm bandpass) and emission (8-nm bandpass) monochromators and interfaced to an Apple-11+ computer. Magic angle polarizers were set to 55° on the excitation side and 0° on the emission side to avoid the Wood's anomaly of the emission grating. Temperature of the cell holder was regulated with a Lauda circulating bath. Spectra were corrected for wavelength-dependent instrument response by using correction factors determined with a standard lamp from Optronics. Fluorescence quantum yields  $\Phi$  were measured at 280-nm excitation wavelength, 25 °C, by comparison to tryptophan (Sigma, recrystallized four times from 70% ethanol) in glass-distilled water. Sample quantum yields were calculated by using a value of 0.14 for tryptophan.<sup>37</sup>

Centers of gravity  $\nu_{cg}$  (in nm<sup>-1</sup>) of emission spectra *I*( $\lambda$ ) were calculated from<sup>38</sup>

$$\nu_{cg} = \frac{\sum_j I(\lambda_j) \lambda_j^{-3}}{\sum_j I(\lambda_j) \lambda_j^{-2}} \quad (1)$$

with the wavelength  $\lambda_j$  taken over the entire emission spectrum in 1-nm intervals.

**Time-Resolved Fluorescence.** Fluorescence decays were collected by time-correlated single photon counting on a Photochemical Research

(26) Wagner, B. D.; James, D. R.; Ware, W. R. *Chem. Phys. Lett.* **1987**, *138*, 181–184.

(27) Donzel, B.; Gauduchon, P.; Wahl, Ph. *J. Am. Chem. Soc.* **1974**, *96*, 801–808.

(28) Petrich, J. W.; Chang, M. C.; McDonald, D. B.; Fleming, G. R. *J. Am. Chem. Soc.* **1983**, *105*, 3824–3832.

(29) Chang, M. C.; Petrich, J. E.; McDonald, D. B.; Fleming, G. R. *J. Am. Chem. Soc.* **1983**, *105*, 3819–3824.

(30) Engh, R. A.; Chen, L. X.-Q.; Fleming, G. R. *Chem. Phys. Lett.* **1986**, *126*, 365–372.

(31) Sipior, J.; Sulkes, M.; Auersbach, R.; Boivineau, M. *J. Phys. Chem.* **1987**, *91*, 2016–2018.

(32) Philips, L. A.; Webb, S. P.; Martinez, S. J., III; Fleming, G. R.; Levy, D. H. *J. Am. Chem. Soc.* **1988**, *110*, 1352–1355.

(33) Dezube, B.; Dobson, C. M.; Teague, C. E. *J. Chem. Soc. Perkin Trans. 2*, **1981**, 730–735.

(34) Cavanaugh, J. R. *J. Am. Chem. Soc.* **1970**, *92*, 1488–1493.

(35) Colucci, W. J.; Tilstra, L.; Sattler, M. C.; Fronczek, F. R.; Barkley, M. D. *J. Am. Chem. Soc.*, following paper in this issue.

(36) Harvey, D. G.; Miller, E. J.; Robson, W. *J. Chem. Soc.* **1941**, 153–159.

(37) Chen, R. F. *Anal. Lett.* **1967**, *1*, 35–42.

(38) Lakowicz, J. R.; Hogen, D. *Biochemistry* **1981**, *20*, 1366–1373.

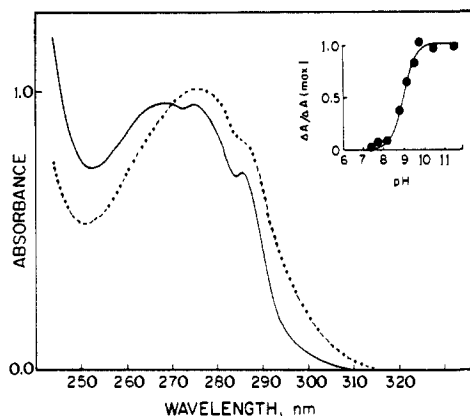


**Figure 1.** Absorption spectra of W(1) zwitterion (—, pH 5.5) and anion (---, pH 10.5) at 25 °C. Inset is a plot of the absorbance change at 278 nm vs pH:  $\Delta A = A(\text{pH } 7.1) - A(\text{pH})$ ;  $\Delta A(\text{max}) = A(\text{pH } 7.1) - A(\text{pH } 11.9)$ .

Associates nanosecond fluorometer interfaced to a Digital Equipment Corp. MINC-11 computer. The excitation source was a flash lamp filled with 1.7 atm  $\text{N}_2$  operated at 24 kHz with  $\sim 6$  kV applied across a 1.5–2.0-mm electrode gap. The width of the instrumental response was 1.7 ns. Excitation wavelength (10-nm bandpass) was selected by a 296-nm interference filter (microCoatings). Emission wavelength (8-nm bandpass) was selected with an Instruments SA H-10 monochromator. Since the incident beam was unpolarized, the polarizer on the emission side was oriented at 35°. Fluorescence decays from a sample and a reference fluorophore were acquired contemporaneously to  $\sim 1.5 \times 10^4$  counts in the peak. The counting rate was less than 2% of the lamp repetition rate. Decay curves were stored in 512 channels of 0.108 ns/channel. A solution of *p*-terphenyl (Aldrich, 99+%) in 75% ethanol and 0.8 M KI (containing a trace of sodium thiosulfate to retard  $\text{I}_3^-$  formation) was used as reference fluorophore. Lifetimes of  $0.27 \pm 0.02$  ns at 5 °C to  $0.18 \pm 0.02$  ns at 45 °C for the quenched terphenyl were determined in separate experiments using *N*-acetyltryptophanamide (Sigma) in 0.01 M phosphate buffer, pH 7.0, as the monoexponential standard. Temperature was regulated with a Lauda circulating bath.

Fluorescence decay data were fitted by reference deconvolution<sup>39</sup> to a sum of exponentials:

$$I(t) = \sum_i \alpha_i \exp(-t/\tau_i) \quad (2)$$

with amplitudes  $\alpha_i$  and lifetimes  $\tau_i$ . Goodness of fit was judged by the magnitude of reduced  $\chi^2$  ( $\chi_r^2$ ) and the shape of the autocorrelation function of the weighted residuals. Decay curves measured at different emission wavelengths were analyzed by a global program,<sup>40</sup> with the constraint that the lifetimes are independent of wavelength. The validity of assumed models for the fluorescence decay was tested by single- and multiple-curve analyses with the reference lifetime fixed.

Decay-associated emission spectra  $I_i(\lambda)$  were calculated from

$$I_i(\lambda) = I(\lambda)\alpha_i(\lambda)\tau_i / \sum_j \alpha_j(\lambda)\tau_j \quad (3)$$

where  $I(\lambda)$  is the corrected steady-state intensity and  $\alpha_i(\lambda)$  is the amplitude of component  $i$  at wavelength  $\lambda$ . Centers of gravity  $\nu_{\text{cg}}$  for steady-state and decay-associated intensities were calculated according to eq 1 with the wavelength taken over the indicated range at 5- or 10-nm intervals.

## Results and Discussion

**Absorbance.** The absorption spectra of the zwitterion and anion forms of W(1) are shown in Figure 1. The spectrum of the zwitterion is structured with peaks at 270 and 276 nm and a smaller peak at 286 nm. Above pH 9.0 the spectrum is smoother, with a peak at 278 nm and a shoulder at 286 nm. The absorption spectrum of the W(1) zwitterion is similar to the spectrum of the tryptophan zwitterion, but the W(1) spectrum is slightly blue-shifted and somewhat broader. In tryptophan the 278-nm peak is higher than the 271-nm peak, whereas in W(1) the two main peaks are about the same height. The pK of the amino group in W(1) was determined from the absorbance change at 278 nm

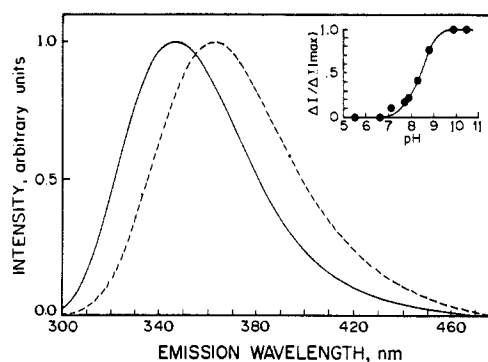


**Figure 2.** Emission spectra of W(1) zwitterion (—, pH 5.5) and anion (---, pH 10.5) at 25 °C. Excitation wavelength 295 nm. Spectra are normalized to the peak.  $\nu_{\text{cg}}^{-1} = 352$  nm for the zwitterion and  $\nu_{\text{cg}}^{-1} = 367$  nm for the anion;  $\nu_{\text{cg}}^{-1}$  is defined in eq 1. Inset is a plot of the intensity change at 345 nm vs pH:  $\Delta I = I(\text{pH } 5.5) - I(\text{pH})$ ;  $\Delta I(\text{max}) = I(\text{pH } 5.5) - I(\text{pH } 10.5)$ .

**Table I.** pH Dependence of W(1) Fluorescence at 25 °C

pH	$\alpha_1(345 \text{ nm})$	$\tau_1, \text{ ns}$	$\tau_2, \text{ ns}$	$\chi_r^2$	$\Phi^a$
5.5		$6.2 \pm 0.1^b$		1.2–1.4	$0.44 \pm 0.02$
7.0		$5.9 \pm 0.2^b$		1.1–1.3	$0.41 \pm 0.02$
8.9		$5.5^c$		1.59	$0.30 \pm 0.01$
8.9	0.49 <sup>c</sup>	$4.7^c$	$6.2^c$	1.15	
10.5		$4.9 \pm 0.2^b$		1.1–1.4	$0.26 \pm 0.02$

<sup>a</sup> 280-nm excitation wavelength. Two to six experiments. <sup>b</sup> 296-nm excitation wavelength. Three to five experiments at 345-nm emission wavelength. <sup>c</sup> 296-nm excitation wavelength. Global analysis of experiments at 5-nm intervals, 320–380-nm emission wavelength.

(inset of Figure 1) by the method of Hermans et al.<sup>41</sup> The pK of W(1) was 8.8 at 25 °C, compared to 9.4 for tryptophan.<sup>41</sup>

**Steady-State Fluorescence.** The steady-state emission spectrum of W(1) is broad and featureless (Figure 2). The emission maximum occurs at 345 nm ( $\nu_{\text{cg}}^{-1} = 352$  nm) in the zwitterion, shifting to 363 nm ( $\nu_{\text{cg}}^{-1} = 367$  nm) in the anion. The fluorescence quantum yield of W(1) decreased with increasing pH from 0.44 at pH 5.5 to 0.26 at pH 10.5 (Table I). Tryptophan also has a broad featureless emission spectrum and a large Stokes shift: the emission maximum of the zwitterion is at 348 nm.<sup>42</sup> However, the quantum yield of the tryptophan zwitterion is only 0.14 at pH 7.0,<sup>37</sup> increasing to 0.31 at pH 10.5.<sup>15</sup>

The pH dependence of the fluorescence intensity of W(1) was monitored at 345-nm emission wavelength in solutions having equal absorbance at the excitation wavelength. The inflection point of the intensity change was around pH 8.5 (inset of Figure 2), which is very near the ground-state pK. The excited-state pK\* of the amino group in W(1) was estimated from the Förster cycle:

$$\text{pK} - \text{pK}^* = Nhc(\bar{\nu}_Z - \bar{\nu}_A) / 2.303RT \quad (4)$$

where  $N$  is Avogadro's number,  $h$  is Planck's constant,  $c$  is the speed of light in the solution,  $R$  is the gas constant,  $T$  is absolute temperature, and  $\bar{\nu}_Z$  and  $\bar{\nu}_A$  are the wavenumbers of the transitions of the zwitterion and anion, respectively. Depending on whether  $\bar{\nu}_Z$  and  $\bar{\nu}_A$  are taken from the absorption maxima, the average of the absorption and emission maxima, or the emission maxima, pK\* is calculated to be 0.7, 1.6, or 2.6 pH units below pK. Tryptophan behaves similarly, with an estimated excited-state pK\*  $\sim 1.5$  pH units smaller than the ground-state pK.<sup>29</sup>

**pH Dependence of Fluorescence Decay.** Table 1 presents fluorescence lifetime data for W(1) at 25 °C and four pH values. At pH 5.5 fluorescence decay curves collected at 345-nm emission wavelength gave acceptable fits to a single exponential with a lifetime of 6.2 ns and  $\chi_r^2$  values of 1.2–1.4. The autocorrelation function fluctuated randomly about zero, and neither the  $\chi_r^2$  value nor the shape of the autocorrelation function improved for dou-

(39) Kolber, Z. S.; Barkley, M. D. *Anal. Biochem.* **1986**, *152*, 6–21.

(40) Knutson, J. R.; Becchem, J. M.; Brand, L. *Chem. Phys. Lett.* **1983**, *102*, 501–507.

(41) Hermans, J., Jr.; Donovan, J. W.; Scheraga, H. A. *J. Biol. Chem.* **1960**, *235*, 91–93.

(42) Teal, F. W. J.; Weber, G. *Biochem. J.* **1957**, *65*, 476–482.

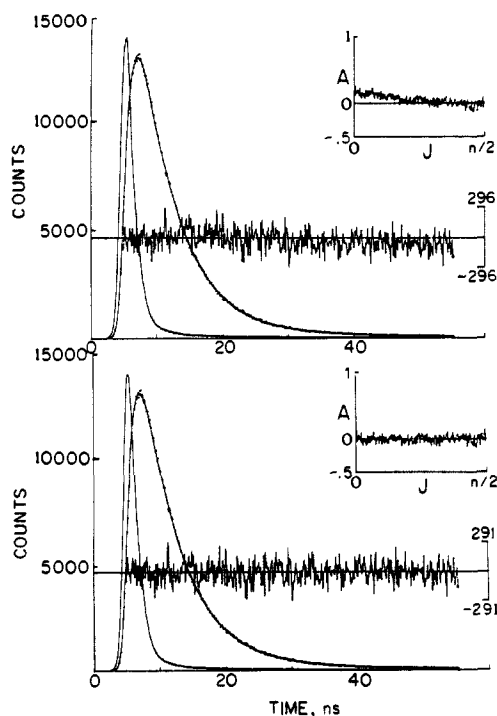


**Figure 3.** Fluorescence decay of W(1) at pH 8.9, 25 °C. Emission wavelength 345 nm. Left curve is reference decay. Points are sample decay; smooth curve through points is best fit to the following: (upper) single-exponential function,  $\tau = 5.5$  ns; partial  $\chi_r^2 = 1.42$  and (lower) double-exponential function,  $\alpha_1 = 0.49$ ,  $\tau_1 = 4.7$  ns,  $\alpha_2 = 0.51$ ,  $\tau_2 = 6.2$  ns; partial  $\chi_r^2 = 1.15$ . Weighted percent residuals and autocorrelation function of the residuals (inset) are also shown.

ble-exponential fits. At pH 7.0 and 10.5 the decays were also single exponentials with  $\chi_r^2$  values in the range 1.1–1.4 and random autocorrelation functions. The lifetime of the zwitterion at pH 7.0 was about the same as at pH 5.5. The lifetime of the anion at pH 10.5 was 4.9 ns. Thus, it appears that the zwitterion and anion forms of W(1) have monoexponential fluorescence decays with slightly different lifetimes. The lifetime of the anion is  $\sim 1$  ns shorter than the lifetime of the zwitterion.

The fluorescence decay of W(1) measured near the pK was clearly biexponential (Figure 3). Proton transfer between nitrogen and oxygen acids and bases in solution is diffusion controlled.<sup>43</sup> The protonation and deprotonation rates of W(1) at pH = pK are estimated to be  $\sim 60$  s<sup>-1</sup>, assuming a bimolecular rate constant of  $4 \times 10^{10}$  M<sup>-1</sup> s<sup>-1</sup> for the protonation reaction. The excited-state deprotonation rate would increase to  $\sim 3 \times 10^4$  s<sup>-1</sup> if pK\* were 2.6 pH units below pK. These proton-transfer rates are slow relative to fluorescence emission, so the biexponential decay should reflect ground-state heterogeneity. Time-resolved emission spectroscopy at pH 8.9 provided evidence that the two lifetimes are due to zwitterion and anion forms of W(1). Decay curves were acquired at 5-nm intervals between 320- and 380-nm emission wavelength and were deconvolved by global analysis. A single-exponential fit gave a lifetime of 5.5 ns, but the global  $\chi_r^2 = 1.6$  and the shape of the autocorrelation function were unsatisfactory (upper panel). The global  $\chi_r^2$  value dropped to 1.2 and the autocorrelation function became more random for a double-exponential fit (lower panel). The two lifetimes of 6.2 and 4.7 ns were essentially identical with the lifetimes of the zwitterion and the anion. Moreover, the decay-associated spectra resembled the emission spectra of the two ionic forms (not shown), with centers of gravity at 344 nm for the 6.2-ns component and 351 nm for the 4.7-ns component. Like the W(1) anion, the 4.7-ns component has a red-shifted emission spectrum.

If the two fluorescence decays represent two ionization states of W(1), then the lifetimes should be independent of pH but the

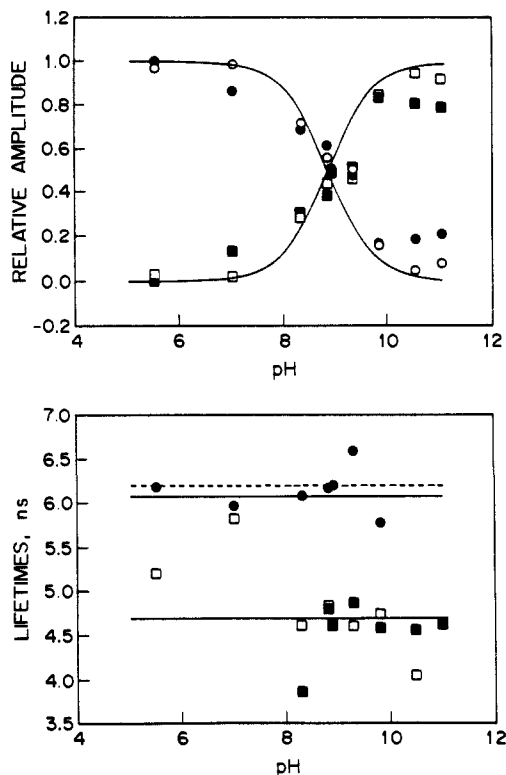


**Figure 4.** pH dependence of fluorescence decay parameters of W(1). Data acquired at 345-nm emission wavelength, 25 °C, were fit to biexponential functions by three methods as described in the text: ( $\square$ ,  $\blacksquare$ ) shorter lifetime component, ( $\circ$ ,  $\bullet$ ) longer lifetime component. Relative amplitudes (upper): ( $\square$ ,  $\circ$ ) method 1, (—, —) method 2, ( $\blacksquare$ ,  $\bullet$ ) method 3. Lifetimes (lower): ( $\square$ , ---) method 1, ( $\blacksquare$ ,  $\bullet$ ) method 2, (—, —) method 3.

amplitudes should depend on the relative concentration of zwitterion and anion. The amplitudes in eq 1 will also be proportional to the molar extinction coefficients  $\epsilon$ , fluorescence intensities  $I$ , and radiative rates  $k_r$  of the zwitterion Z and anion A.

$$\alpha_A/\alpha_Z = \epsilon_A I_A k_{r,A}[A] / \epsilon_Z I_Z k_{r,Z}[Z] \quad (5)$$

Decay curves were collected at 345-nm emission wavelength over the pH range 5.5–11.3. The data were fit to double exponentials by three methods: (1) single-curve analysis with one lifetime fixed at 6.2 ns, (2) single-curve, linked-function analysis<sup>44</sup> with the amplitude ratio fixed according to eq 5, and (3) global analysis with the two lifetimes constrained to be independent of pH. In computing the amplitude ratios, the relative extinction coefficient  $\epsilon_A/\epsilon_Z$  was determined from the ratio of the absorbance of solutions at pH 5.5 and 10.5 containing equal concentrations of W(1). The absorbance was averaged between 291 and 301 nm to mimic the excitation filter used in the nanosecond fluorometer. The relative intensity  $I_A/I_Z$  at 345 nm was calculated from the emission spectra of the same solutions. The ratio of the radiative rates was estimated from the quantum yields and lifetimes according to eq 10. Substituting the numerical values into eq 5 gives

$$\alpha_A/\alpha_Z = (1.8)(0.54)(0.81)[A]/[Z] \quad (6)$$

The value of  $[A]/[Z]$  at a given pH was calculated from the Henderson–Hasselbalch equation.

$$\text{pH} - \text{pK} = \log [A]/[Z] \quad (7)$$

Figure 4 depicts the results obtained from the three types of data analysis. The upper panel plots the relative amplitudes while the lower panel plots the lifetimes of the two decays as a function of pH. In all cases, the amplitudes show the expected pH depen-

(43) Crooks, J. E. In *Proton-Transfer Reactions*; Caldin, E. F., Gold, V., Eds.; Chapman and Hall: London, 1975; Chapter 6.

(44) Ross, J. B. A.; Laws, W. R.; Sutherland, J. C.; Buku, A.; Katsoyannis, P. G.; Schwartz, J. L.; Wyssbrod, H. R. *Photochem. Photobiol.* **1986**, *44*, 365–370.

**Table II.** Comparison of Fluorescence Data for W(1) and Tryptophan

	$\alpha_1(330 \text{ nm})$	$\tau_1, \text{ ns}$	$\tau_2, \text{ ns}$	$\Phi$
W(1) <sup>a</sup>				
pH 7.0		5.9 ± 0.2		0.41 ± 0.02
pH 10.5		4.9 ± 0.2		0.26 ± 0.02
tryptophan <sup>b</sup>				
pH 7	0.32	0.53 ± 0.05	3.13 ± 0.03	0.14
pH 10.5	0.45	4.55 ± 0.4	10.1 ± 0.4	0.31

<sup>a</sup>Data from Table I at 25 °C. <sup>b</sup>Data from ref 15 at 20 °C.

dence: the amplitude of the shorter lifetime component (squares) grows with increasing pH at the expense of the longer lifetime component (circles). The lifetimes appear to be independent of pH. Method 1 treats the amplitudes and shorter lifetime as free parameters and fixes the longer lifetime at 6.2 ns (lower panel; broken line). It recovers amplitudes (upper panel, open symbols) in excellent agreement with the values calculated from eqs 6 and 7 (upper panel, solid lines). Most of the lifetimes obtained for the shorter component (lower panel, open squares) are close to the value for the anion (Table I). Method 2 treats both lifetimes as free parameters and fixes the amplitude ratio on the basis of the relative concentrations of zwitterion and anion. The solid lines in the upper panel of Figure 4 show the pH dependence of the calculated amplitudes. The two curves cross at pH 8.9. The lifetimes (lower panel, filled symbols) fluctuate around the expected values for the zwitterion and anion in the range 7.0 < pH < 10.5. Attempts to fit the data for lower and higher pH to biexponential functions were unsuccessful because one amplitude was near zero. Method 3 links the lifetimes in a multiple-curve analysis and leaves the amplitudes unrestricted. The values recovered for the amplitudes (upper panel, filled symbols) parallel the amplitudes from method 1. The 6.08- and 4.70-ns lifetimes (lower panel, solid lines) agree very well with the values for the zwitterion and anion given in Table I. Although there is some scatter of the points in Figure 4, the overall agreement between the three methods of data analysis is quite good, especially considering the difficulty of resolving two such closely spaced decays. This affirms the presence of two ionic forms in solution whose relative concentration is dependent on pH.

In contrast to tryptophan, W(1) appears to have a single-exponential decay except near the pK. Table II summarizes the fluorescence lifetime data for the zwitterion and anion forms of both compounds. Tryptophan has a double-exponential decay at acidic and neutral pH with a third component appearing around pH 9.0.<sup>18,45</sup> The simplified fluorescence decay of the W(1) zwitterion is probably a result of restricting rotation of the alanyl side chain. Furthermore, the lifetime of the W(1) anion is ~1 ns shorter than the zwitterion lifetime and remains almost constant to pH 11.3, the highest pH measured. In tryptophan, the anion lifetime is much longer than the zwitterion lifetimes but decreases above pH 10.5.<sup>17,46</sup> The increased lifetime of the deprotonated forms of both tryptophan<sup>46</sup> and tryptamine<sup>28</sup> is undoubtedly due to suppression of the excited-state intramolecular proton transfer.<sup>23,24,47</sup> The conformational constraint in W(1) precludes the assistance of proton exchange at C4 of indole by the positively charged amine.<sup>35</sup>

**Temperature Dependence of Fluorescence Decay.** The temperature dependence of the fluorescence lifetime informs about nonradiative routes for deactivation of the excited state. The fluorescence decay of the W(1) zwitterion was measured over the temperature range 5–45 °C. Table III summarizes the results of global analysis of time-resolved emission spectral data collected at 5, 25, and 45 °C. The global analyses of data sets for pH 5.5 and 7.0 gave acceptable fits to monoexponential decays with temperature-dependent lifetime. Two closely spaced lifetimes

**Table III.** Time-Resolved Emission Spectral Data for W(1) Zwitterion<sup>a</sup>

pH	<i>t</i> , °C	$\alpha_1(340 \text{ nm})$	$\tau_1, \text{ ns}$	$\tau_2, \text{ ns}$	$\chi_r^2$	$\nu_{\text{cg}}^{-1}, \text{ nm}$	
						1	2
5.5	5 <sup>b</sup>	0.29	7.23	7.40	1.18	343	345
			6.79		1.24		
			6.15		1.14		
7.0	5 <sup>c</sup>	0.23	5.38	6.31	1.17	341	341
			4.67		1.15		
			3.86		1.19		
7.0	25 <sup>f</sup>	0.05	7.13	7.34	1.45	343	350
			6.18		1.14		
			5.92		1.16		
7.0	45 <sup>d</sup>	0.20	5.37	6.03	1.12	339	339

<sup>a</sup>Global analysis of experiments at 5-nm intervals. <sup>b</sup>320–385 nm. <sup>c</sup>10-nm intervals, 320–370 nm. <sup>d</sup>320–370 nm. <sup>e</sup>315–390 nm. <sup>f</sup>315–370 nm.

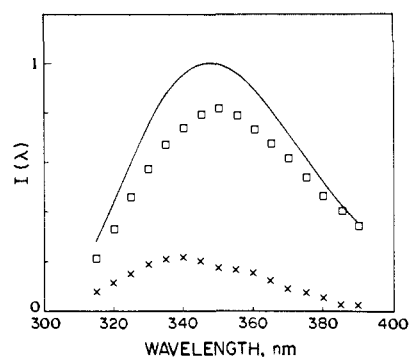


**Figure 5.** Decay-associated emission spectra of W(1) at pH 7.0, 5 °C. Excitation wavelength 296 nm. (—) steady-state emission spectrum,  $\nu_{\text{cg}}^{-1} = 350 \text{ nm}$ ; (□) 7.3-ns component,  $\nu_{\text{cg}}^{-1} = 350 \text{ nm}$ ; (×) 6.2-ns component,  $\nu_{\text{cg}}^{-1} = 343 \text{ nm}$ .

could be resolved in double-exponential fits with little or no change in  $\chi_r^2$  or randomness of the autocorrelation function. The resolution of a biexponential decay for the W(1) zwitterion was most convincing in the data set acquired at pH 7.0, 5 °C. Here the global  $\chi_r^2$  dropped from 1.5 for the single-exponential fit to 1.1 for the double-exponential fit and the autocorrelation functions indicated a slight improvement in the fit to two exponentials. Moreover, the decay-associated emission spectra of the two lifetime components were clearly separated (Figure 5). The spectrum of the 6.2-ns component lies slightly to the blue of the spectrum of the 7.4-ns component. The spectral separation at 5 °C is also evident from the centers of gravity of the decay-associated emission spectra given in Table III. In the preceding case of the double-exponential decay obtained near the pK of W(1), the shorter lifetime component was associated with a red-shifted emission spectrum. The observation of different spectral associations in a pH range well below the pK argues that the biexponential decays at pH 5.5 and 7.0 are not due to two ionization states of W(1). The longer lifetime component contributes ~80% of the total fluorescence emission. As discussed in the companion paper,<sup>35</sup> the two fluorescence lifetimes probably represent the two conformations available to W(1). We achieve better resolution of the closely spaced biexponential decays in subsequent experiments using a picosecond dye laser excitation source.

The fluorescence lifetime is determined by the rates of radiative  $k_r$  and nonradiative  $k_{nr}$  processes

$$\tau^{-1} = k_r + k_{nr} \quad (8)$$

where the nonradiative rate  $k_{nr}$  includes both temperature-independent and temperature-dependent pathways. The total temperature-independent rate  $k_0$  is assumed to comprise the radiative  $k_r$  and intersystem crossing  $k_{isc}$  rates.<sup>48,49</sup>

$$k_0 = k_r + k_{isc} \quad (9)$$

(45) Leismann, H.; Scharf, H.-D.; Strassburger, W.; Wollmer, A. *J. Photochem.* **1983**, *21*, 275–280.

(46) De Lauder, W. B.; Wahl, Ph. *Biochemistry* **1970**, *9*, 2750–2754.

(47) Shizuka, H.; Serizawa, M.; Kobayashi, H.; Kameta, K.; Sugiyama, H.; Maisuura, T.; Saito, I. *J. Am. Chem. Soc.* **1988**, *110*, 1726–1732.

(48) Feitelson, J. *Isr. J. Chem.* **1970**, *8*, 241–252.

**Table IV.** Temperature Dependence of the Single-Exponential Fit of W(1) Fluorescence Decay Data, pH 7.0.

<i>t</i> , °C	$\tau$ , <sup>a</sup> ns	$\chi_r^2$	<i>t</i> , °C	$\tau$ , <sup>a</sup> ns	$\chi_r^2$
5	7.13 <sup>b</sup>	1.45	30	5.55 ± 0.01	1.06–1.11
10	6.88 ± 0.01	1.19–1.30	35	5.16 ± 0.01	1.14–1.24
15	6.57 ± 0.01	1.10–1.14	40	4.81 ± 0.10	1.15–1.17
20	6.24 ± 0.02	1.14–1.17	45	4.3 ± 0.1	1.17–1.19
25	5.89 <sup>b</sup>	1.16			

<sup>a</sup> Three experiments at 345-nm emission wavelength. <sup>b</sup> Data from Table III.

The radiative rate  $k_r$  can be calculated from the quantum yield  $\Phi$  and observed lifetime  $\tau$

$$k_r = \Phi/\tau \quad (10)$$

From the data in Table I for W(1) at pH 5.5 and 10.5, the radiative rate of the zwitterion is  $k_r = 7.1 \times 10^7 \text{ s}^{-1}$ , ~34% faster than the radiative rate of the anion,  $k_r = 5.3 \times 10^7 \text{ s}^{-1}$ . Protonation of the amino group in tryptophan likewise increases the radiative rate by a factor of 1.26.<sup>29</sup> The radiative rates of the zwitterion and anion forms of W(1) are slightly faster than the corresponding rates in tryptophan. Chang et al.<sup>29</sup> estimated radiative rates of  $6.3 \times 10^7$  and  $5.0 \times 10^7 \text{ s}^{-1}$  for tryptophan derivatives with and without a protonated amino group. The radiative rates for tryptophan calculated from the data of Szabo and Rayner<sup>15</sup> cited in Table II are  $4.8 \times 10^7 \text{ s}^{-1}$  at pH 7 and  $3.1 \times 10^7 \text{ s}^{-1}$  at pH 10.5. Szabo and Rayner<sup>15</sup> also reported quantum yields and lifetimes for a variety of tryptophan derivatives at pH 7. These data give a radiative rate of  $5.5 \times 10^7 \text{ s}^{-1}$  for tryptamine, compared to values of  $(4.1\text{--}4.5) \times 10^7 \text{ s}^{-1}$  for analogues lacking a protonated amino group. The presence of a positively charged amine appears to cause small enhancements of the radiative rate in tryptophan derivatives.

The temperature-dependent nonradiative rate of the indole chromophore is usually represented by a single Arrhenius factor. In this case, eq 8 becomes

$$\tau^{-1} = k_0 + A \exp[-E^*/RT] \quad (11)$$

where  $A$  is the frequency factor and  $E^*$  is the activation energy. Not knowing the intersystem crossing rate of W(1), we must analyze the temperature dependence of the fluorescence lifetime by choosing a plausible value for  $k_0$  in the Arrhenius plot or by curve-fitting directly to eq 11. To estimate the temperature-independent rate  $k_0$  we assume that the intersystem crossing rate is the same in W(1) and 2,3-dimethylindole. Lipert et al.<sup>50</sup> determined  $k_{\text{isc}} = 2.8 \times 10^7 \text{ s}^{-1}$  from the intersystem crossing quantum yield and the singlet decay rate of 2,3-dimethylindole in a supersonic free jet. An order of magnitude lower value of  $0.36 \times 10^7 \text{ s}^{-1}$  was deduced from the temperature-independent portion of the nonradiative rate of aqueous 2,3-dimethylindole.<sup>51</sup> With this assumption, the  $k_0$  values calculated from eq 9 are in the range  $(7.5\text{--}9.9) \times 10^7 \text{ s}^{-1}$ .

Fluorescence decay curves for W(1) at pH 7.0 were collected at 5 °C intervals from 5 to 45 °C and were fit to single-exponential functions (Table IV). A plot of  $\ln(\tau^{-1} - k_0)$  vs  $(RT)^{-1}$  using the high estimate of  $k_0 = 9.9 \times 10^7 \text{ s}^{-1}$  is shown in Figure 6a. The slope and intercept of the least-squares line give values of  $A = 3.2 \times 10^{11} \text{ s}^{-1}$  and  $E^* = 5.0 \text{ kcal/mol}$ . However, the Arrhenius plot is slightly curved. A nonlinear least-squares fit of the lifetime data to eq 11 gives  $k_0 = 1.25 \times 10^8 \text{ s}^{-1}$ ,  $A = 3.7 \times 10^{13} \text{ s}^{-1}$ , and  $E^* = 8.1 \text{ kcal/mol}$  (Figure 6b). The poor agreement between the two procedures suggests that there is more than one temperature-dependent process in the fluorescence decay of W(1). For example, the two lifetime components resolved by global analysis might have somewhat different temperature dependences. Alternatively, we may have picked an erroneous value of  $k_0$  to construct the Arrhenius plot. If we take the low estimate of  $k_0$

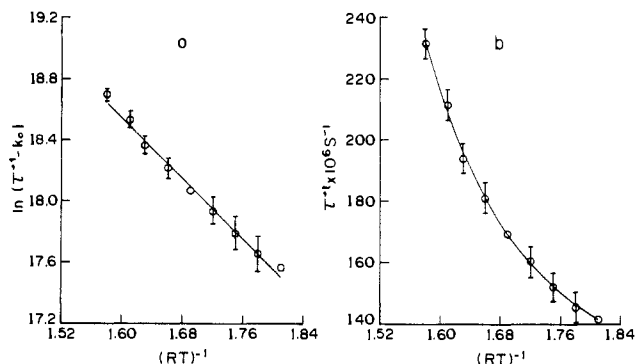


**Figure 6.** Fit of temperature dependence of fluorescence lifetime of W(1) at pH 7.0 to Arrhenius equation. (a) Linear least-squares fit of data to  $\ln(\tau^{-1} - k_0) = \ln A - E^*/RT$ , assuming  $k_0 = 9.9 \times 10^7 \text{ s}^{-1}$ . (b) Nonlinear least-squares fit of data to  $\tau^{-1} = k_0 + A \exp(-E^*/RT)$ .

$= 7.5 \times 10^7 \text{ s}^{-1}$ , the plot of  $\ln(\tau^{-1} - k_0)$  vs  $(RT)^{-1}$  shows larger deviations from linearity. However, putting back in the value  $k_0 = 2.25 \times 10^8 \text{ s}^{-1}$  obtained from the nonlinear fit of eq 11 produces a linear Arrhenius plot and excellent agreement in the values of  $A = 4.0 \times 10^{13} \text{ s}^{-1}$  and  $E^* = 8.1 \text{ kcal/mol}$ . Such a large  $k_0$  value implies that the intersystem crossing rate of W(1) is  $k_{\text{isc}} = 5.4 \times 10^7 \text{ s}^{-1}$ , almost as fast as the radiative rate. These two possibilities will be discussed further in the companion paper.<sup>35</sup> Chang et al.<sup>29</sup> obtained frequency factors of  $(2\text{--}12) \times 10^{13} \text{ s}^{-1}$  and activation energies of 6.7 kcal/mol for the major and minor lifetime components of the tryptophan zwitterion. In constructing the Arrhenius plots for each component, they assumed a temperature-independent rate of  $9.9 \times 10^7 \text{ s}^{-1}$ , which is identical with our high estimate but slightly greater than their previous estimates<sup>17</sup> of  $\sim 8 \times 10^7 \text{ s}^{-1}$  for 3-methylindole and tryptophan anion. Recently, Boens et al.<sup>20</sup> repeated the temperature study of the tryptophan zwitterion using a one-step global analysis of decay curves acquired at three emission wavelengths as a function of temperature. They found the same values for the Arrhenius parameters of the major lifetime component:  $k_0 = 1 \times 10^8 \text{ s}^{-1}$ ,  $A = 3 \times 10^{13} \text{ s}^{-1}$ , and  $E^* = 6.7 \text{ kcal/mol}$ . However, the sub-nanosecond decay of the minor lifetime component was independent of temperature with  $k_0 = 1.4 \times 10^9 \text{ s}^{-1}$ .

## Conclusions

The results for the constrained tryptophan derivative W(1) provide strong support for the conformer model of tryptophan photophysics. Limiting the rotational freedom of the alanyl side chain clearly inhibits a nonradiative decay pathway that occurs in the tryptophan zwitterion. Since the conformational restriction simplifies the fluorescence decay, two-state excited-state reactions and other models unrelated to rotamers cannot account for the complex decay of tryptophan. The constrained derivative W(1) appears to have a single-exponential fluorescence decay. As shown in the companion paper,<sup>35</sup> W(1) adopts two half-chair conformations in solution. The apparent monoexponential decay implies either that the lifetimes of the two conformers are similar or that the conformers interconvert rapidly compared to the fluorescence time scale. A double-exponential decay with two closely spaced lifetimes can be resolved by global analysis of time-resolved emission spectral data.

Besides the conformational restriction, W(1) differs from tryptophan in having an additional methylene substituent on the indole ring. Although we expect the extra methylene to perturb the electronic states, we do not believe that it will influence the complexity of the fluorescence decay. The effects of methyl substitution on the photophysics are best understood for gas-phase indoles. The lowest excited electronic state of indole derivatives in the gas phase is  $^1L_b$ .<sup>32,52</sup> Methyl substitution of indole reduces the  $^1L_b\text{--}^1L_a$  energy gap<sup>4</sup> and shortens the fluorescence lifetime of the bare molecule. In a free jet expansion, the lifetimes of

(49) Klein, R.; Tatischeff, I. *Chem. Phys. Lett.* **1977**, *51*, 333–338.

(50) Lipert, R. J.; Bermudez, G.; Colson, S. D. *J. Phys. Chem.* **1988**, *92*, 3801–3805.

(51) Glasser, N.; Lami, H. *J. Mol. Struct.* **1986**, *142*, 193–196.

(52) Hager, J. W.; Demmer, D. R.; Wallace, S. C. *J. Phys. Chem.* **1987**, *91*, 1375–1382.

indole, 3-methylindole, 2,3-dimethylindole, and 1,2,3,4-tetrahydrocarbazole are 17.5, 13.5, 6.0, and 3.9 ns, respectively.<sup>52</sup> The latter compound is a W(1) analogue, which lacks the amino acid functional groups. The intersystem crossing rate in isolated indoles is relatively insensitive to methyl substitution, being  $1.7 \times 10^7$ ,  $2.5 \times 10^7$ , and  $2.8 \times 10^7$  s<sup>-1</sup> for indole, 3-methylindole, and 2,3-dimethylindole.<sup>50</sup> The substantial drop of the fluorescence lifetime in the 2,3-dialkylindoles has been attributed to N-H bond rupture caused by coupling of the bound <sup>1</sup>L<sub>b</sub> state with a dissociative <sup>1</sup>L<sub>a</sub> state.<sup>52</sup> The N-H dissociation pathway may also make a small contribution to the nonradiative decay of indole in nonpolar solvents,<sup>53</sup> but there is no evidence for it in polar solvents.<sup>12</sup>

Less is known about the solution photophysics of methyl-substituted indoles. The lowest excited electronic state of most indole derivatives is <sup>1</sup>L<sub>b</sub> in nonpolar and rigid polar solvents, but <sup>1</sup>L<sub>a</sub> in polar fluid media.<sup>4</sup> However, in 2,3-dimethylindole <sup>1</sup>L<sub>a</sub> is the lowest excited state even in nonpolar solvents.<sup>54</sup> In aqueous solution at 20 °C, indole, 3-methylindole, and 2,3-dimethylindole have monoexponential decays with lifetimes of 4.8, 9.4, and 4.3 ns.<sup>6,14,15,55</sup> The lifetime of 3-methylindole is independent of pH

over the range pH 3-11.<sup>17</sup> The radiative rates calculated from quantum yield and lifetime data are  $(4.8-5.2) \times 10^7$  s<sup>-1</sup> for indole,<sup>14,15</sup>  $(3.1-5.0) \times 10^7$  s<sup>-1</sup> for 3-methylindole,<sup>6,15,17,56</sup> and  $3.5 \times 10^7$  s<sup>-1</sup> for 2,3-dimethylindole.<sup>13,55</sup> The estimated intersystem crossing rate is equal to the radiative rate in aqueous indole<sup>12</sup> and  $\sim 3.3 \times 10^7$  s<sup>-1</sup> in 3-methylindole.<sup>17</sup> W(1) is a 2,3-dialkylindole. Although the zwitterion has a somewhat longer lifetime than aqueous 2,3-dimethylindole, the 4.9-ns lifetime of the anion approaches the lifetime of 2,3-dimethylindole. This is opposite to the trend in tryptophan, where the zwitterion lifetimes are much shorter than the lifetime of 3-methylindole and the anion lifetime is about the same as 3-methylindole.<sup>17</sup> The complex fluorescence decays observed in many 3-substituted indoles are due to the functional groups on the alkyl side chain,<sup>15,28,57</sup> not the alkane moiety.

**Acknowledgment.** This work was supported by NIH grant GM35009.

**Registry No.** W, 73-22-3; W(1), 42438-90-4.

(53) Pernot, C.; Lindqvist, L. *J. Photochem.* **1976/1977**, *6*, 215-220.  
(54) Strickland, E. H.; Billups, C.; Kay, E. *Biochemistry* **1972**, *11*, 3657-3662.

(55) Keating-Nakamoto, S. M.; Cherek, H.; Lakowicz, J. R. *Biophys. Chem.* **1986**, *24*, 79-95.  
(56) Meech, S. R.; Phillips, D.; Lee, A. G. *Chem. Phys.* **1983**, *80*, 317-328.  
(57) James, D. R.; Ware, W. R. *J. Phys. Chem.* **1985**, *89*, 5450-5458.

## Conformational Studies of a Constrained Tryptophan Derivative: Implications for the Fluorescence Quenching Mechanism

William J. Colucci,<sup>†</sup> Luanne Tilstra,<sup>‡</sup> Melissa C. Sattler,<sup>§</sup> Frank R. Fronczek, and Mary D. Barkley\*

Contribution from the Department of Chemistry, Louisiana State University, Baton Rouge, Louisiana 70803-1804. Received May 18, 1990. Revised Manuscript Received August 10, 1990

**Abstract:** The ground-state conformation of a rotationally constrained tryptophan derivative, 3-carboxy-1,2,3,4-tetrahydro-2-carboline, W(1), is determined from single-crystal X-ray diffraction, MM2 calculations, and <sup>1</sup>H NMR coupling constants. The solid-state structure represents the predominant solution conformation. W(1) populates only two minimum-energy conformations in solution, which correspond to the half-chair forms of cyclohexene. The conformers are distinguished mainly by distance of the carboxylate from the indole ring. The MM2-computed barrier for ring inversion in W(1) is 5.91 kcal/mol. The constrained tryptophan derivative and its ethyl ester, W(1)E, are used to investigate nonradiative decay pathways in tryptophan photophysics. The conformational restriction eliminates the excited-state intramolecular proton-transfer reaction observed with tryptophan (Saito, I.; Sugiyama, H.; Yamamoto, A.; Muramatsu, S.; Matsuura, T. *J. Am. Chem. Soc.* **1984**, *106*, 4286-4287). Global analysis of time-resolved fluorescence data reveals biexponential decays with lifetimes of 3.6 and 6.3 ns for the W(1) zwitterion and 2.9 and 4.8 ns for the W(1) anion. The relative amplitudes ( $\alpha_1 = 0.12-0.20$  and  $\alpha_2 = 0.88-0.80$ ) match the relative populations of the two conformers (0.3 and 0.7). Consequently, one lifetime is assigned to each conformer. The shorter lifetime component is associated with the conformer having the carboxylate closest to the indole ring. Esterification replaces the carboxylate of W(1) with a better electron acceptor and shortens both lifetimes, suggesting that intramolecular electron transfer may be an important mode of quenching. Arrhenius parameters confer that the temperature-dependent nonradiative process occurring in W(1) and W(1)E probably involves electron transfer.

Although the fluorescence of tryptophan is widely studied, its photophysics is not fully understood.<sup>1,2</sup> Numerous explanations have been proposed for the complex fluorescence decays of the tryptophan zwitterion as well as individual tryptophans in peptides and proteins. Several models for the biexponential decay of the tryptophan zwitterion are described in the preceding paper.<sup>3</sup>

Among these the conformer model, which presumes emission from distinct, noninterconverting rotamers, is most frequently discussed.<sup>4-7</sup> Two nonradiative decay processes, intramolecular

<sup>†</sup> Present address: Ethyl Corp., Ethyl Technical Center, 8000 GSR I Ave., Baton Rouge, La 70820.

<sup>‡</sup> Present address: NIST, Bldg. 224, Rm. B-320, Gaithersburg, MD 20899.

<sup>§</sup> Present address: Dow Chemical USA, R&D Bldg. 2503, Box 400, Plaquemine, LA 70765-0400.

(1) Creed, D. *Photochem. Photobiol.* **1984**, *39*, 537-562.  
(2) Beechem, J. M.; Brand, L. *Annu. Rev. Biochem.* **1985**, *54*, 43-71.  
(3) Tilstra, L.; Sattler, M. C.; Cherry, W. R.; Barkley, M. D. *J. Am. Chem. Soc.*, preceding paper in this issue.  
(4) Szabo, A. G.; Rayner, D. M. *J. Am. Chem. Soc.* **1980**, *102*, 554-563.  
(5) Chang, M. C.; Petrich, J. W.; McDonald, D. B.; Fleming, G. R. *J. Am. Chem. Soc.* **1983**, *105*, 3819-3824.  
(6) Petrich, J. W.; Chang, M. C.; McDonald, D. B.; Fleming, G. R. *J. Am. Chem. Soc.* **1983**, *105*, 3824-3832.